

TMAO Induces Vascular Endothelial Cells Pyroptosis Through TET2-CYTB-ROS Pathway

Linzhen Xia¹⁻³, Zuo Wang², Xiangyu Chen^{1,3}

¹Molecular Pathology Laboratory, Department of Pathology, Changsha Hospital for Maternal and Child Health Care, Hunan Normal University, Changsha, Hunan, People's Republic of China; ²Institute of Cardiovascular Disease, Key Laboratory for Arteriosclerosis of Hunan Province, Hunan International Scientific and Technological Cooperation Base of Arteriosclerotic Disease, Department of Bioinformatics and Medical Big Data, Hengyang Medical School, University of South China, Hengyang, Hunan, People's Republic of China; ³Hunan Provincial Key Laboratory of Regional Hereditary Birth Defects Prevention and Control, Changsha Hospital for Maternal and Child Care, Hunan Normal University, Changsha, Hunan, People's Republic of China

Correspondence: Zuo Wang, Institute of Cardiovascular Disease, Key Laboratory for Arteriosclerosis of Hunan Province, Hunan International Scientific and Technological Cooperation Base of Arteriosclerotic Disease, Department of Bioinformatics and Medical Big Data, Hengyang Medical School, University of South China, Hengyang, Hunan, People's Republic of China, Tel +86 17773459876, Email smt121101@163.com; Xiangyu Chen, Molecular pathology laboratory, Department of Pathology, Changsha Hospital for Maternal and Child Health Care, Hunan Normal University, Changsha, Hunan, People's Republic of China, Tel +86 18175102867, Email chenxiangyu@cssfybjy.com

Purpose: The study was aimed at identifying that cytochrome b (CYTB) expression regulation by trimethylamine N-oxide (TMAO) can induce mitochondria reactive oxygen species (ROS) and promote vascular endothelial cells (VECs) pyroptosis.

Methods: VECs were transfected with TET methylcytosine dioxygenase 2 (TET2)/CYTB overexpression lentivirus, CYTB siRNA, TET2 shRNA, or NC. ROS levels were measured using MitoSOX Red fluorescence, and pyroptosis was evaluated via Hoechst 33342/PI staining. Western blot was used to measure TET2, the NOD-like receptor thermal protein domain associated protein 3 (NLRP3), proteolytic cleavage of gasdermin D (GSDMD), CYTB, and Caspase-1 expression. Interleukin (IL)-1 β was quantified by ELISA. The mRNA expression of IL-1 β , CYTB, ND2, and TET2 was measured by qRT-PCR. Cellular ultrastructure was examined by electron microscope, and calcium flux was monitored with Fluo-4AM. CYTB methylation was detected using Targeted Bisulfite Sequencing.

Results: This study showed that TMAO can down-regulate the expression of CYTB in VECs, cause VECs pyroptosis and mitochondrial dysfunction (MDF). CYTB overexpression antagonized the effect of TMAO. Further, silencing CYTB promoted mtROS production, and MitoTEMPO, a ROS scavenger, inhibited VECs pyroptosis caused by CYTB silencing. In addition, TET2 had demethylation activity. The expression of CYTB was positively regulated by TET2. TMAO was able to inhibit the expression of TET2 and promote the methylation level of the CYTB gene promoter.

Conclusion: TMAO promotes the methylation level of the CYTB gene promoter and down-regulates the expression of CYTB by inhibiting the expression of TET2. The decreased expression level of CYTB induces ROS, promoting VECs pyroptosis.

Keywords: atherosclerosis, pyroptosis, mitochondrial dysfunction, trimethylamine N-oxide, cytochrome b

Introduction

Atherosclerosis (AS) is a leading cause of death in developed countries and is considered a form of chronic inflammation.¹ Atherosclerotic cardiovascular disease (ASCVD), especially ischaemic heart disease and ischaemic stroke, is the leading cause of morbidity and mortality globally.² In 2021, ischaemic heart disease and ischaemic stroke caused about 9.37 million deaths, representing about 13.72% of all deaths around the world.³ In China, ASCVD caused 2.4 million deaths in 2016, representing 25% of all deaths.⁴ Atherosclerosis is characterized by the deposition of fibrous tissues and lipids in the intima of elastic arteries, leading to thrombus formation and the thickening and hardening of vessel walls, ultimately causing structural damage.⁵ Cell death and inflammation play critical roles at various stages of atherosclerosis.⁶ Pyroptosis, an inflammatory form of programmed cell death, is induced by caspase-1/4/5/11. It is characterized by cell swelling, plasma membrane lysis, chromatin fragmentation and the release of inflammatory substances such as interleukin (IL)-1 β and IL-18.⁷⁻⁹ Proteolytic cleavage of gasdermin D (GSDMD) by Caspase-1/4/5/11, leading to membrane perforation and rupture, plays an important role in pyroptosis.¹⁰⁻¹²

Trimethylamine N-oxide (TMAO), an endothelial-toxic factor produced by gut flora from phosphatidylcholine in meat, participates in foam cell formation and plaque growth in animal models,^{13–15} and is closely related to vascular endothelial cells (VECs) pyroptosis.^{16,17} It induces inflammation and endothelial dysfunction through reactive oxygen species (ROS) generation.¹⁸ Mitochondria are the source of most ROS,¹⁹ and mitochondrial dysfunction (MDF) promoted ROS production, which activated the NOD-like receptor thermal protein domain associated protein 3 (NLRP3) inflammasome, leading to pyroptosis of VECs.^{20,21} Cytochrome b (CYTB), encoded by mitochondrial DNA (mtDNA), is a key component of complex III in the mitochondrial oxidative phosphorylation system and serves as one of the cytopigments for electron transport in the mitochondrial respiratory chain.^{22,23} The decreased expression of CYTB leads to the disorder of complex III formation,^{24,25} which inhibits the electron transport in respiratory chain and increases ROS production in mitochondria.²⁶ The *CYTB* mutations can lead to NLRP3 inflammasome activation, apoptosis, endothelial dysfunction and atherosclerosis.^{27–33} Tet methylcytosine dioxygenase2 (TET2) is a demethylating enzyme that catalyze the conversion of 5-methylcytosine (5-mC) in DNA to 5-hydroxylMethylcytosine (5-hmC).³⁴ Our previous studies have shown that silencing TET2 can induce pyroptosis of VECs by promoting ROS production in VECs.^{35,36}

The study was aimed to validate the hypothesis that TMAO promoted VECs pyroptosis via the TET2-CYTB-ROS pathway. In this study, the effect of TMAO on the pyroptosis of VECs, intracellular TET2 and CYTB expression, and ROS levels, was investigated, and the underlying mechanism by which TET2, CYTB and ROS regulated TMAO-induced VECs pyroptosis by inducing MDF was explored.

Materials and Methods

Cell Culture and Transfection

VECs were obtained from Science Cell Research Laboratories (Carlsbad, CA) and cultured in VEC medium containing 10% fetal bovine serum in a humidified atmosphere at 37°C, 5% CO₂, and 95% air. TET2 overexpression and short hairpin RNA (shRNA) lentiviruses, CYTB overexpression lentivirus, and the negative control (NC) were synthesized by GeneChem (Shanghai, China). CYTB small interfering RNA (CYTBsiRNA: GCAACACTCCACCTCCTAT) and NC were purchased from RiboBio (Guangzhou, China). VECs were transfected with CYTBsiRNA or NC using riboFECTTM CP Transfection Kit, and transfection efficiency was evaluated with protein expression by Western blot analysis. Transfection of TET2 overexpression/shRNA lentivirus, CYTB overexpression lentivirus or NC was conducted using HitransG of GeneChem (Shanghai, China), and transfection efficiency was assessed by observing fluorescence under a fluorescence microscope.

Measurement of ROS Levels

To distinguish from TET2 and CYTB exhibiting green fluorescence, MitoSOX Red fluorescence probe (M36008, Thermo Fisher Scientific) was used for ROS fluorescence detection. The cells were washed twice with cold phosphate-buffered saline (PBS, pH 7.4) and incubated with MitoSOX (5 µM) for 30 minutes in the dark at 37°C. Diamidino-2-phenylindole (DAPI) (10 µg/mL, C0065, Beijing Solarbio Science & Technology) was used for counterstaining for 10 minutes in the dark at room temperature. The cells were then observed under an Olympus IX3 fluorescence microscope (Olympus, Tokyo, Japan).

Western Blot

Cells were washed three times with ice-cold PBS and lysed on ice for 30 minutes with radioimmunoprecipitation assay buffer (RIPA) containing phenylmethanesulfonyl fluoride (PMSF) at a 94:6 ratio. The cells were then collected and centrifuged at 12,000 rpm for 10 minutes at 4°C. Protein concentration in the supernatant was measured using a BCA protein assay kit. A 20 µg protein sample per well was loaded onto an 8–12% sodium dodecyl sulfate polyacrylamide gel, then transferred to a nitrocellulose membrane and blocked with PBS containing 5% nonfat milk for 2 hours. The membrane was incubated with TET2 (1:1,000; Proteintech, Rosemont), NLRP3 (1:500; Proteintech, Rosemont), GSDMD (1:500; Proteintech, Rosemont), CYTB (1:500; Proteintech, Rosemont), Caspase-1 (1:500; Proteintech, Rosemont), Pro-caspase-1 (1:1000; Proteintech), GSDMD-N (1:1000; Proteintech, Rosemont) and diluted in TBST containing 2.5% skim milk buffer at 4°C overnight. After

the membranes were washed five times with PBS containing Tween 20, the membranes were incubated with fluorescence-conjugated anti-rabbit IgG secondary antibody (1:2000) at room temperature for 1.5 hours. Glyceraldehyde 3-phosphate dehydrogenase (GAPDH) (Proteintech) was used as a loading control. Quantity One Software was used to visualize the protein bands, and the target protein was quantified.

Enzyme-linked Immunosorbent Assay

Enzyme-linked immunosorbent assay (ELISA) was performed to measure the levels of IL-1 β secretion in VECs. After treatment, the cell supernatant was collected, and 100 μ L of the sample were taken for ELISA analysis according to the manufacturer's protocol (NeoBioscience, Guangzhou, China).

Quantitative reverse-transcription polymerase chain reaction

Total RNA was extracted from VECs using Trizol reagent and then reverse transcribed into cDNA using RT kit (TOYOBO). The ABI 7000 sequence detection system was used, and SYBR Green Premix Dimer Eraser (Takara) was used for quantitative PCR. RNA levels were normalized using *GAPDH* specific primers. The primer sequences used for quantitative reverse-transcription polymerase chain reaction (qRT-PCR) were as follows:

IL-1 β forward, 5'-CGATCACTGAACTGCACG CT-3' and reverse, 5'-AGAACACCACTTGTGCTCCA-3'; CYTB forward, 5'-TATGGCTGAATCATCCGCTAC3' and reverse, 5'-GGATAATGCCGATGTTTC-3'; NADH dehydrogenase subunit 2 (ND2) forward, 5'-AATAAACCCCTCGTTCCAC-3' and reverse, 5'-CTGGGACTCAGAAGTGAAAGG-3'; and TET2 forward, 5'-CAAAATCAAGCGAGTTCGAGA-3' and reverse, 5'-ATGCACTTGATTTCATGGTC-3'; GAPDH forward, 5'-AAG ATCAAGATCATTGCTCCTCCTG-3' and reverse, 5'-GCCGGACTCGTCATACTCCT-3';

Scanning and Transmission Electron Microscope

After the cells were digested with trypsin, they were collected by centrifugation at 1000 rpm for 10 minutes and fixed with phosphate-buffered glutaraldehyde. Scanning electron microscopy was performed using a HT-7700 electron microscope (Tokyo, Japan), and transmission electron microscopy was performed using a H7650 electron microscope (Tokyo, Japan).

Calcium Ion Measurement

Fluo-4AM was stored and diluted to a 2.5 μ M working solution in an EP tube, protected from light. The cells were washed three times with PBS to remove phenol red, which may affect the background color. Next, the Fluo-4AM working solution was added, and the cells were incubated for 30 minutes in a 37°C water bath. Finally, the cells were washed three times with PBS and then observed under a fluorescence microscope (IX3, Olympus).

Hoechst 33342/PI Staining

Hoechst 33342/propidium iodide (PI) staining was used to evaluate pyroptosis. The VECs were rinsed three times with phosphate-buffered solution (PBS) and then incubated in the dark at 37°C for 10 minutes with Hoechst 33342 solution. After removing the dye, the cells were washed with PBS, PI dye was added, and the cells were incubated for 10 minutes in the dark at 37°C. After washing three times with PBS, the cells were observed under a fluorescence microscope (IX3, Olympus).

Bioinformatics Analysis

The following websites were used for CpG island analysis: MethPrimer (<http://www.urogene.org/methprimer2/>) and the UCSC Genome Browser.

Targeted Bisulfite Sequencing

Targeted Bisulfite Sequencing (TBS) combines traditional Bisulfite Sequencing PCR (BSP) with high-throughput sequencing to enable methylation detection and verification for multiple CpG sites or target regions. First, BS-PCR primers were designed and synthesized based on the target region or site ([Supplementary Table 1](#)). Next, DNA was extracted, quality-controlled, and treated with bisulfite using the EZ DNA Methylation Gold Kit (Zymo Research). Following bisulfite

treatment, unmethylated cytosines (C) were converted to uracils (U), which were later amplified as thymine (T) during PCR, while methylated cytosines remained unchanged. The bisulfite-treated template was then amplified using high-fidelity U-base-tolerant DNA polymerase. BSP amplification products from the same sample were pooled together, and amplification with tag primers was performed using Illumina sequencing adapters. Finally, sequencing libraries with distinct tags for each sample were prepared, purified, quantified, mixed, and quality-checked before sequencing.

Statistical Analysis

Data were expressed as mean \pm SD and analyzed using one-way analysis of variance (ANOVA) followed by the Newman-Keuls multiple comparison test (GraphPad Prism Version 5.0, CA). Two groups were compared using a two-tailed Student's *t*-test, and $P < 0.05$ was considered statistically significant.

Results

TMAO Induces VECs Pyroptosis

TMAO is an endothelial toxic factor produced by intestinal flora and is closely related to VECs dysfunction.³⁷ To investigate the relationship between TMAO and VECs pyroptosis, we performed in vitro experiments using VECs. After incubating VECs with 600 $\mu\text{mol/L}$ TMAO for 24 hours,³⁸ the expression levels of NLRP3, GSDMD, Pro-caspase-1, Caspase-1, and both the protein and mRNA levels of the proinflammatory cytokine IL-1 β were significantly increased (Figure 1A–C). During pyroptosis, pores formed in the cell membrane, resulting in the release of cellular contents, which can be determined by PI staining.³⁹ PI could not penetrate an intact cell membrane but is able to enter damaged membranes, resulting in red staining of the nucleus. Pyroptosis in VECs was detected by Hoechst 33342 and PI staining, which showed that TMAO induced pore formation and membrane rupture, characterized by an increase in extensive PI positive staining (Figure 1D). Scanning electron microscopy showed that the VECs membrane was ruptured, showing the appearance of membrane pores on the cell membrane (Figure 1E). These results collectively confirmed that TMAO induced VEC pyroptosis.

TMAO Induces VECs Mitochondrial Dysfunction

Intracellular ROS is mainly produced by MDF, and the increase of mitochondrial ROS can directly lead to cell pyroptosis.⁴⁰ In order to further explore the effects of TMAO on mitochondrial structure and function in VECs, the expression of Nuclear Respiratory Factor 1 (NRF1), NRF2, and Peroxisome Proliferator-Activated Receptor- γ Coactivator-1 α (PGC-1 α) at the protein level, along with the expression of ND2 at the mRNA level, was measured. The results of qRT-PCR and Western blot analysis showed that TMAO could decrease the mitochondrial gene level (Figure 2A and B). Transmission electron microscopy showed abnormal morphological changes of mitochondria, as revealed by shortened cristae and vesicular structure formation (Figure 2C). In order to verify whether the cells pyroptosis caused by TMAO is realized by MDF, ROS in VECs was detected by MitoSOX probe, and the results showed that ROS increased under TMAO conditions (Figure 2D). Fluo-4 AM results also suggested that TMAO may be associated with an increase in calcium influx (Figure 2E). The above results indicated that TMAO induced VECs pyroptosis and damaged the function of mitochondria.

TMAO Downregulates CYTB Expression

Next, VECs were incubated under TMAO conditions to observe the effect on CYTB expression. Under TMAO treatment, the expression levels of CYTB at both the protein and mRNA levels were significantly decreased (Figure 3A and B). These results indicated that TMAO treatment inhibited CYTB expression.

CYTB Silence Promotes VECs Pyroptosis and MDF

CYTB is a protein that constitutes complex III of the mitochondrial oxidative phosphorylation system and is also involved in electron transfer within the mitochondrial respiratory chain.²² Mutations in genes encoding respiratory chain subunit proteins can alter cell metabolism and potentially lead to tumorigenesis.⁴¹ To observe the relationship between CYTB and VECs

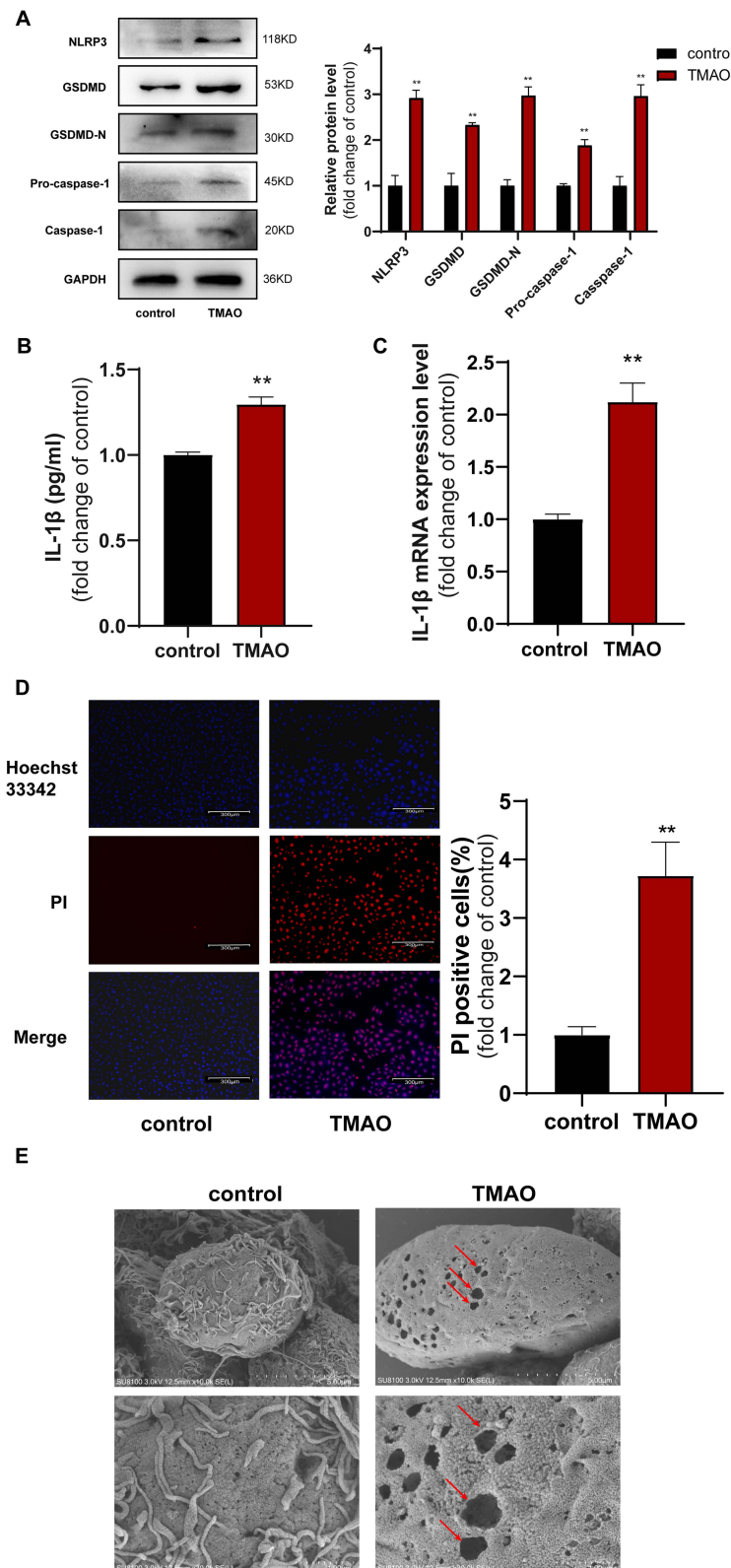


Figure 1 TMAO induces VECs pyroptosis: **(A)** The protein levels of NLRP3, GSDMD, Pro-caspase-I, GSDMD-N and Caspase-I were upregulated in VECs after treatment with 600 $\mu\text{mol/L}$ TMAO for 24 hours, as indicated by Western blot results. GAPDH was used as an internal control. ** $P < 0.01$ versus control group. **(B)** IL-1 β production in the medium was increased after treatment TMAO for 24 hours. ** $P < 0.01$ versus control group. **(C)** The percentage of PI (Red)- positive cells were increased in VECs after treatment with TMAO for 24 hours. scale bar = 300 μm . ** $P < 0.01$ versus control group. **(D)** Statistical analyses of IL-1 β expression in the mRNA level after TMAO treatment of VECs, ** $P < 0.01$ versus control group. Data of statistical analyses are presented as the Mean \pm SD of three independent experiments. **(E)** The membrane of VECs treated with TMAO was observed by scanning electron microscope. The red arrow indicates the pore of the cell membrane. (Scale bar = 5 μm ; 1 μm).

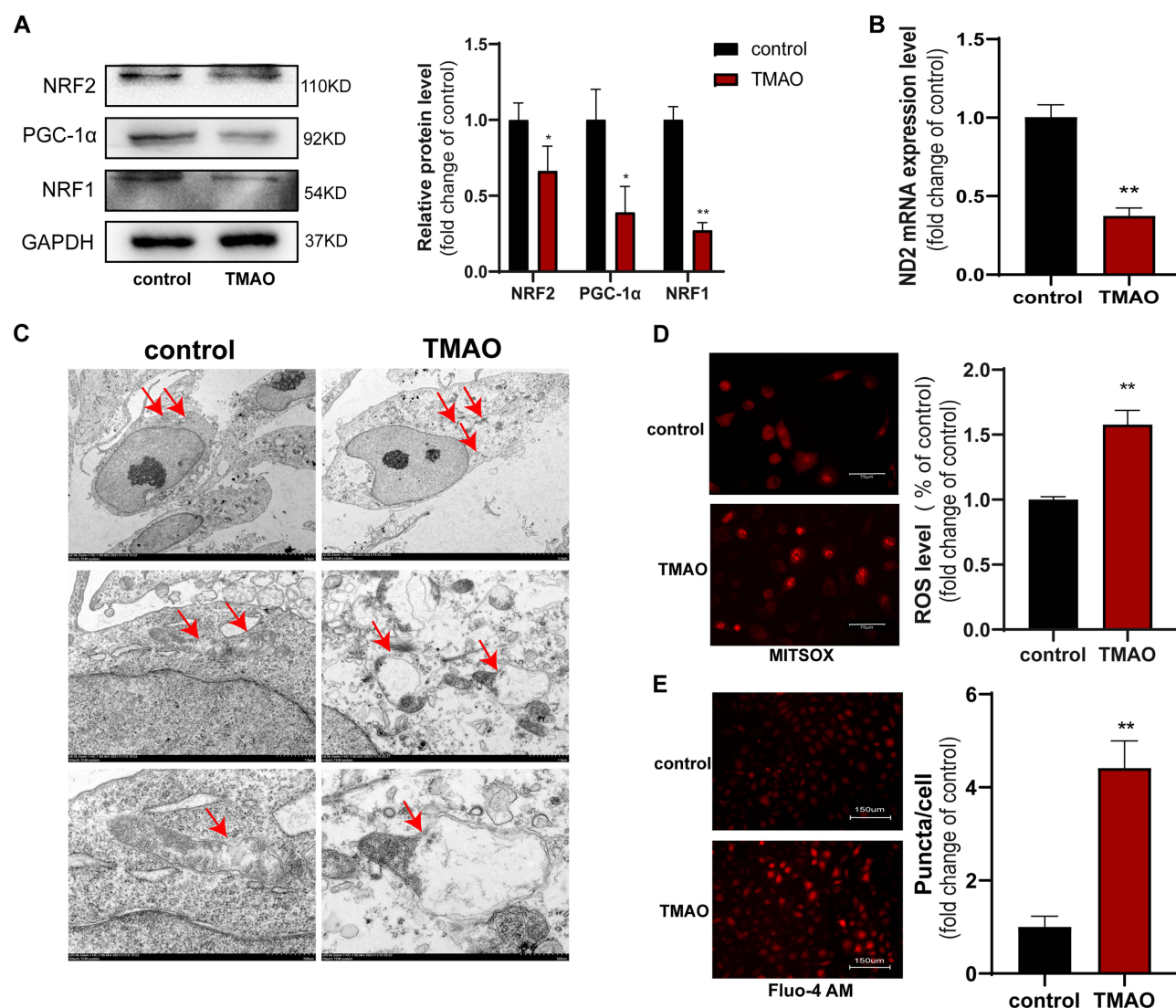


Figure 2 TMAO induces VECs MDF: **(A)** Expression of NRF2, PGC-1α, NRF1 decreased in the TMAO (600 μmol/L) group. GAPDH was used as an internal control. * $P < 0.05$, ** $P < 0.01$ versus control group. **(B)** Statistical analyses of ND2 expression in the mRNA level after TMAO treatment of VECs, ** $P < 0.01$ versus control group. **(C)** Cellular ROS level was detected by MitoSOX and observed (Red) under fluorescence microscope. scale bar = 75 μm. Data of statistical analyses are presented as the mean \pm SD of three independent experiments. ** $P < 0.01$ versus control group. **(D)** Electron microscopy of the mitochondria of TMAO-treated VECs. The red arrows represent mitochondria. (Scale bar = 5 μm; 1 μm; 500 nm.) **(E)** The calcium levels in mitochondria were determined using the probe Fluo-4 AM with immuno- fluorescence detection. Scale bar = 150 μm.

pyroptosis, we knocked down CYTB using CYTBsiRNA. Western blot analysis confirmed that CYTB knockdown was effective (Figure 4A). MitoTEMPO, a mitochondria-targeted antioxidant with superoxide and alkyl radical scavenging properties, was used to determine the role of ROS in VECs pyroptosis. Following CYTB knockdown, VECs were pretreated with MitoTEMPO. The results clearly showed that the increased expression of pyroptosis markers, including NLRP3, Pro-caspase-1, GSDMD, Caspase-1, and GSDMD-N, was inhibited after MitoTEMPO treatment (Figure 4B). The IL-1β levels in the medium transfection with CYTBsiRNA-treated VECs were decreased after pretreatment with MitoTEMPO (Figure 4C). After pretreatment with MitoTEMPO, the mRNA expression of IL-1β, the level of intracellular calcium and the percentage of PI positive cells in VECs treated with CYTBsiRNA decreased, while the mRNA expression of CYTB and ND2 increased (Figure 4D–F). In addition, ROS levels were detected using the ROS species probe (Red), and the fluorescence results showed that ROS levels increased when CYTB expression was knocked down, but ROS levels were inhibited by MitoTEMPO (Figure 4G). These findings supported that CYTB was involved in TMAO-induced VECs pyroptosis through a ROS-dependent mechanism, which may be closely related to mitochondrial function.

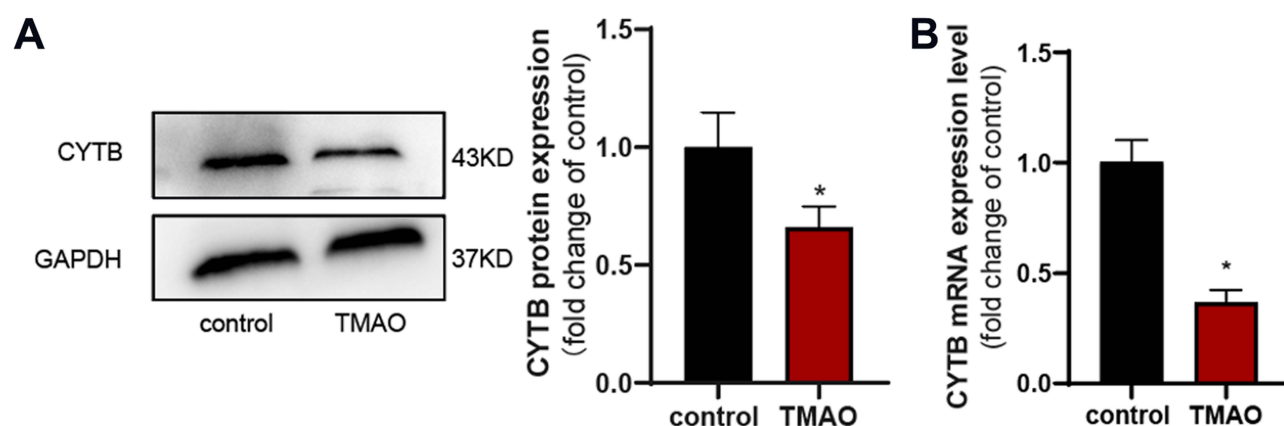


Figure 3 TMAO downregulates CYTB expression: **(A)** The protein level of CYTB was decreased in VECs after treatment with 600 $\mu\text{mol/L}$ TMAO for 24 hours, as indicated by Western blot results. GAPDH was used as an internal control. $*P < 0.05$ versus control group. **(B)** Statistical analyses of CYTB expression in the mRNA level after TMAO treatment of VECs, $*P < 0.05$ versus control group. Data of statistical analyses are presented as the Mean \pm SD of three independent experiments.

CYTB Overexpression Eliminates TMAO Induced VECs Pyroptosis and MDF

To determine the role of CYTB in TMAO-induced VECs pyroptosis, we overexpressed CYTB in VECs and assessed the efficiency (Figure 5A). The results showed that NLRP3, GSDMD, GSDMD-N, Pro-caspase-1, and Caspase-1 were upregulated under TMAO conditions, but their expression was inhibited in the TMAO + OECYTB group (Figure 5B). The results demonstrated that the mRNA levels of CYTB and ND2 decreased under TMAO treatment, but significantly increased in the TMAO + OECYTB group (Figure 5C). Additionally, the protein and mRNA levels of IL-1 β (Figure 5C and D), the percentage of PI-positive cells (Figure 5E), ROS levels (Figure 5F), and intracellular calcium concentrations (Figure 5G) all showed marked increases under TMAO conditions, indicating enhanced pyroptosis and oxidative stress. However, these parameters were significantly reduced in the TMAO + OECYTB group, suggesting that OECYTB mitigated the effects of TMAO. Taken together, these results suggested that CYTB can suppress pyroptosis in VECs and effectively reduce ROS production induced by TMAO, thereby protecting against oxidative stress and inflammation.

TMAO Downregulates TET2 Expression

VECs were incubated under TMAO conditions to observe the effect on TET2 expression. Under TMAO treatment, the expression of TET2 at both the protein and mRNA levels were significantly decreased (Figure 6A and B). Therefore, TMAO treatment inhibited TET2 expression.

TET2 Upregulates CYTB Expression

TET2 plays an important role in DNA methylation.^{42–44} In order to clarify the relationship between TET2 and CYTB, we observed the effect of TET2 knockdown and overexpression on CYTB. The results showed that the expression of CYTB at protein level and mRNA level was decreased after knockout of TET2, while both protein and mRNA levels of CYTB were increased following TET2 overexpression (Figure 7A and B). These results suggested that TET2 can regulate the expression of CYTB.

TMAO Increases the Methylation Level of CYTB Promoter

Through bioinformatics analysis, a CpG island was found in the *CYTB* gene (Figure 8A). As previously mentioned, TBS analyzes the methylation level of the *CYTB* gene and to assess the methylation status of CpG islands in the *CYTB* region after TMAO treatment. Fifteen CpG sites on the *CYTB* gene were selected for detection (Supplementary Table 2). The results showed that the total average methylation level of fifteen CpG sites in the promoter region of the *CYTB* gene was higher in the TMAO group compared to the control group (Figure 8B). Specifically, the methylation level of CpG6 (14804) in the promoter

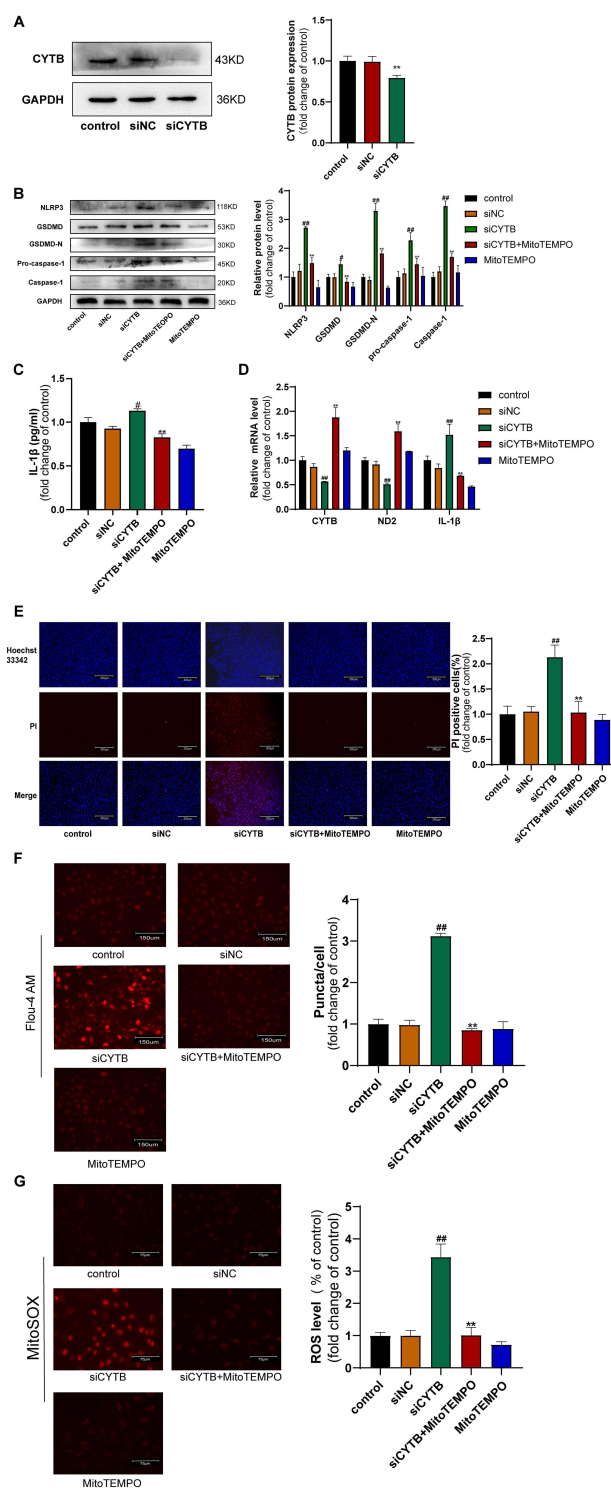


Figure 4 CYTB silence promotes VECs pyroptosis and MDF: **(A)** Transfection efficiency was determined by Western blot for analysis of CYTB expression. The protein level of CYTB is decreased in VECs after transfection with CYTBsiRNA. siNC: negative control. $^{**}P < 0.01$ versus control group. **(B)** MitoTEMPO pretreatment 12 hours suppressed the upregulation of NLRP3, GSDMD, Pro-caspase-1, GSDMD-N and Caspase-1 protein levels after transfection with CYTBsiRNA. $^{#}P < 0.05$; $^{###}P < 0.01$ versus control group; $^{**}P < 0.01$ versus siCYTB group. **(C)** The IL-1 β levels in the medium transfection with CYTBsiRNA-treated VECs was decreased after pretreatment with MitoTEMPO. $^{#}P < 0.05$ versus control group; $^{**}P < 0.01$ versus siCYTB group. **(D)** Statistical analyses of CYTB and ND2 expression in the mRNA level transfection with CYTBsiRNA-treated VECs were increased after pretreatment with MitoTEMPO; the mRNA expression of IL-1 β decreased. $^{###}P < 0.01$ versus control group; $^{**}P < 0.01$ versus siCYTB group. **(E)** The percentage of PI-positive cells was declined after pretreatment with MitoTEMPO in CYTBsiRNA-treated VECs. scale bar = 300 μ m. $^{##}P < 0.01$ versus control group; $^{**}P < 0.01$ versus siCYTB group. **(F)** After pretreatment with MitoTEMPO, the calcium level of VECs treated with CYTBsiRNA decreased. scale bar = 150 μ m. $^{###}P < 0.01$ versus control group; $^{**}P < 0.01$ versus siCYTB group. All results are expressed as the mean \pm SD of three independent experiment. **(G)** CYTBsiRNA increased intracellular ROS level of VECs and this increase was inhibited by MitoTEMPO (5 mM). scale bar = 75 μ m. $^{#}P < 0.01$ versus control group; $^{**}P < 0.01$ versus siCYTB group.

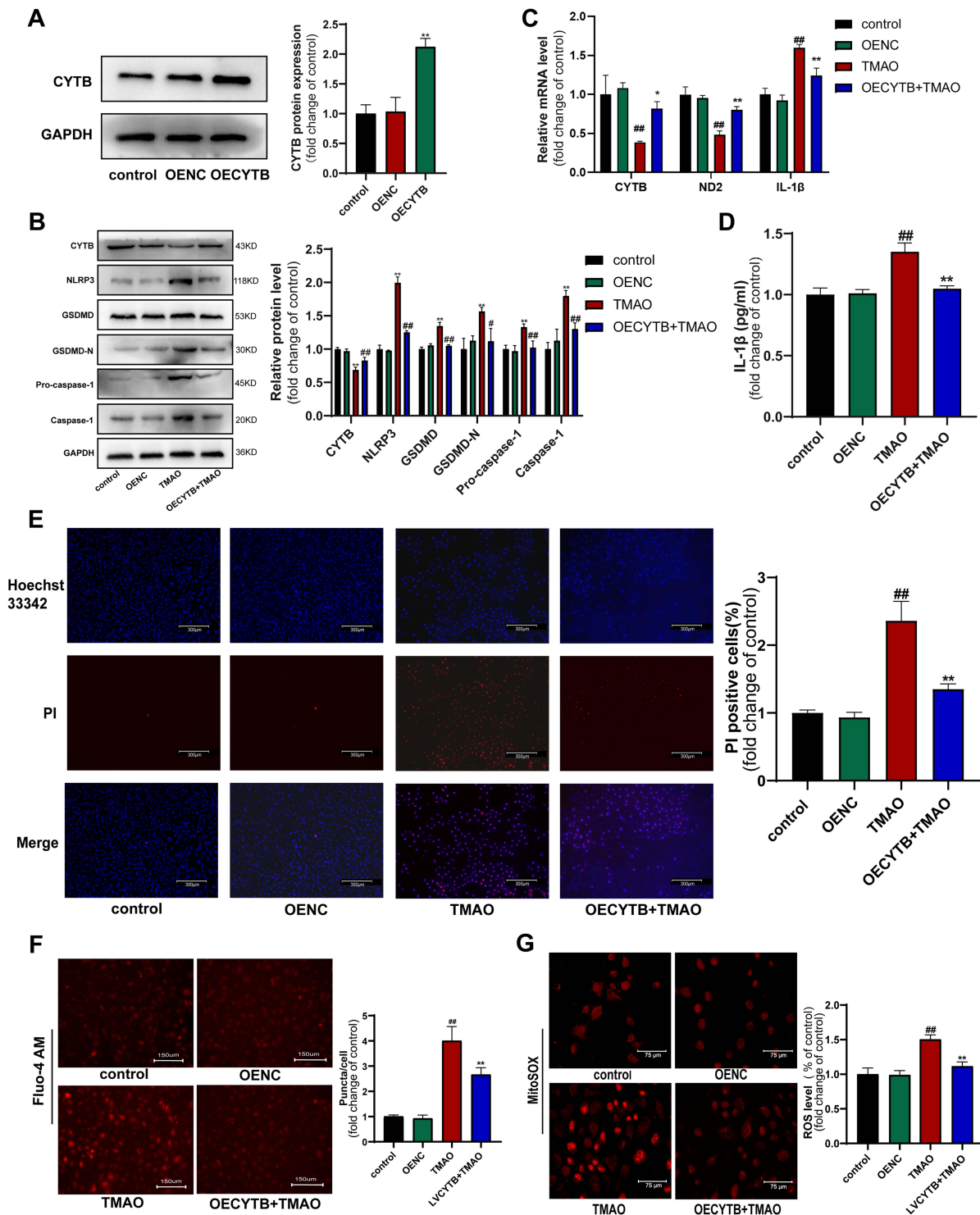


Figure 5 CYTB overexpression eliminates TMAO induced VECs pyroptosis and MDF: **(A)** lentivirus transfection efficiency was determined by Western blot for analysis of CYTB expression. The protein level of CYTB is increased in VECs after transfection of CYTB overexpression lentivirus. $^{**}P < 0.01$ versus control group. **(B)** The protein levels of NLRP3, GSDMD, Pro-caspase-1, GSDMD-N and Caspase-1 in TMAO-treated VECs were decreased and CYTB is increased after transfection of CYTB overexpression lentivirus. $^{###}P < 0.01$ versus control group; $^{*}P < 0.05$; $^{**}P < 0.01$ versus TMAO treatment group. **(C)** The IL-1 β levels in the medium in TMAO-treated VECs were decreased after transfection of CYTB overexpression lentivirus. $^{###}P < 0.01$ versus control group; $^{**}P < 0.01$ versus TMAO treatment group. **(D)** Statistical analyses of CYTB and ND2 expression in the mRNA level in TMAO-treated VECs were increased after transfection of CYTB overexpression lentivirus; the expression of IL-1 β decreased. $^{###}P < 0.01$ versus control group; $^{*}P < 0.05$; $^{**}P < 0.01$ versus TMAO treatment group. **(E)** CYTB overexpression of lentivirus decreased the percentage of PI positive cells in VECs treated with TMAO. scale bar = 300 μ m. $^{###}P < 0.01$ versus control group; $^{**}P < 0.01$ versus TMAO treatment group. **(F)** TMAO increased intracellular ROS level of VECs and this increase was inhibited by CYTB overexpression lentivirus. scale bar = 75 μ m. $^{###}P < 0.01$ versus control group; $^{**}P < 0.01$ versus TMAO treatment group. **(G)** After transfection of CYTB overexpression lentivirus, the calcium level of VECs treated with TMAO decreased. scale bar = 150 μ m. $^{###}P < 0.01$ versus control group; $^{**}P < 0.01$ versus TMAO treatment group. All results are expressed as the mean \pm SD of three independent experiment.

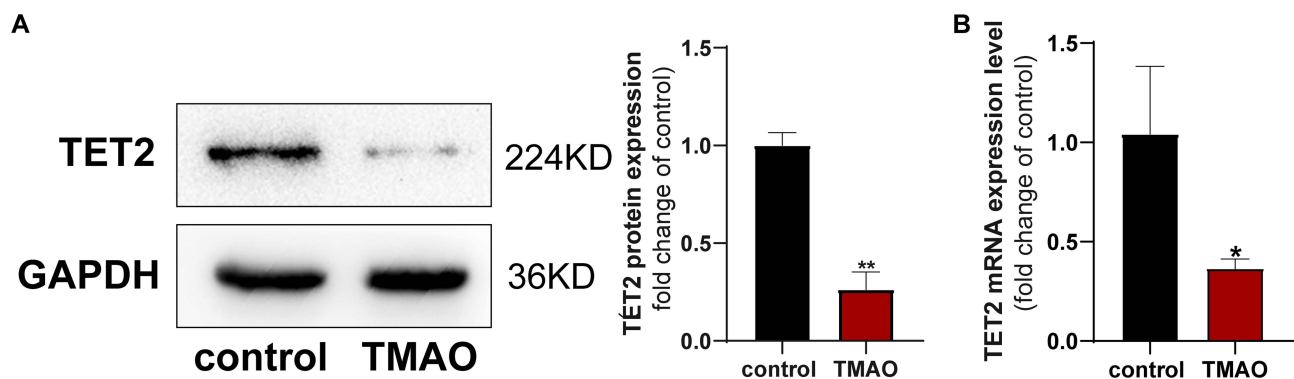


Figure 6 TMAO downregulates TET2 expression: **(A)** The protein level of TET2 was decreased in VECs after treatment with 600 $\mu\text{mol/L}$ TMAO for 24 hours, as indicated by Western blot results, GAPDH was used as an internal control. $^{**}P < 0.01$ versus control group. **(B)** Statistical analyses of TET2 expression in the mRNA level after TMAO treatment of VECs, $^{*}P < 0.05$ versus control group. Data of statistical analyses are presented as the Mean \pm SD of three independent experiments.

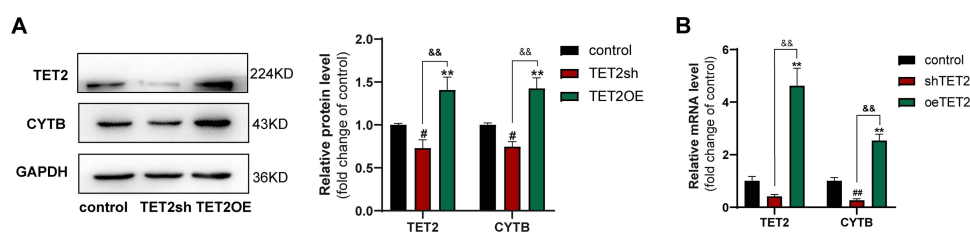


Figure 7 TET2 upregulates CYTB expression: **(A)** Overexpression/interrupted TET2 can change CYTB expression, whereas TET2 overexpression increased CYTB protein level, but decreased when TET2 was interrupted. $^{\#}P < 0.05$ versus control group. $^{**}P < 0.01$ versus shTET2 group. **(B)** Overexpression/interrupted TET2 can regulate the expression of CYTB at mRNA level. $^{###}P < 0.01$ versus control group. $^{**}P < 0.01$ versus shTET2 group.

region was significantly higher in the TMAO group than in the control group (Figure 8C). Therefore, the expression of the *CYTB* gene was regulated through methylation, and TMAO treatment can increase *CYTB* methylation.

Discussion

AS is a chronic inflammatory disease accompanied by cell death and pro-inflammatory cytokine release.⁴⁵ Pyroptosis is a programmed inflammatory mode of cell death,⁴⁶ which is closely related to cardiovascular disease.⁴⁷ TMAO, an intestinal microbial metabolite, is strongly linked to cellular dysfunction in AS.^{48,49} It is primarily derived from choline, found in red meat, fish, poultry, eggs and other foods. Gut microbiota metabolizes choline to trimethylamine, which is further metabolized to TMAO by the hepatic enzyme flavin monooxygenase 3.^{50,51} It promotes VECs pyroptosis through ROS upregulation, thereby contributing to the progression of AS.¹⁷ Lopez-Pastrana et al reported that VECs pyroptosis promoted the release of adhesion molecules, which triggering monocyte adhesion.⁵² This phenomenon facilitates monocyte migration and atherosclerotic lesion progression via the ROS-NLRP3 pathway.⁵³ Consistent with these findings, our results showed that TMAO induced VECs pyroptosis by increasing ROS. Mitochondria, serving as the cell's energy source and essential for maintaining cell homeostasis, is closely related to VECs pyroptosis.²¹ The most ROS are produced by mitochondria, especially those with destroyed mitochondrial homeostasis.⁵⁴

CYTB, encoded by mtDNA (Supplementary Figure 1), is a hydrophobic membrane protein composed of eight transmembrane helices.⁵⁵ The protein is involved in regulation of oxidoreductase activity, metal ion transfer, and electron transport in the respiratory chain.⁵⁶ ROS can drive beneficial homeostasis by coordinating intracellular signaling pathways, and it can also destroy some cellular components and lead to cell death.⁵⁷ Previously, the research on CYTB mainly focused on the *CYTB* gene polymorphisms and mutations that related to numerous clinical presentations including mitochondrial encephalopathy, cardiomyopathy, hypertension, eppto-optic dysplasia and multi-system disorder.^{58–65} Some studies found that *CYTB* gene mutations were associated with NLRP3-inflammasome activation,²⁷ ROS production,⁶⁶ apoptosis,^{28,33} endothelial dysfunction and AS.^{29,67} This study found that the VECs

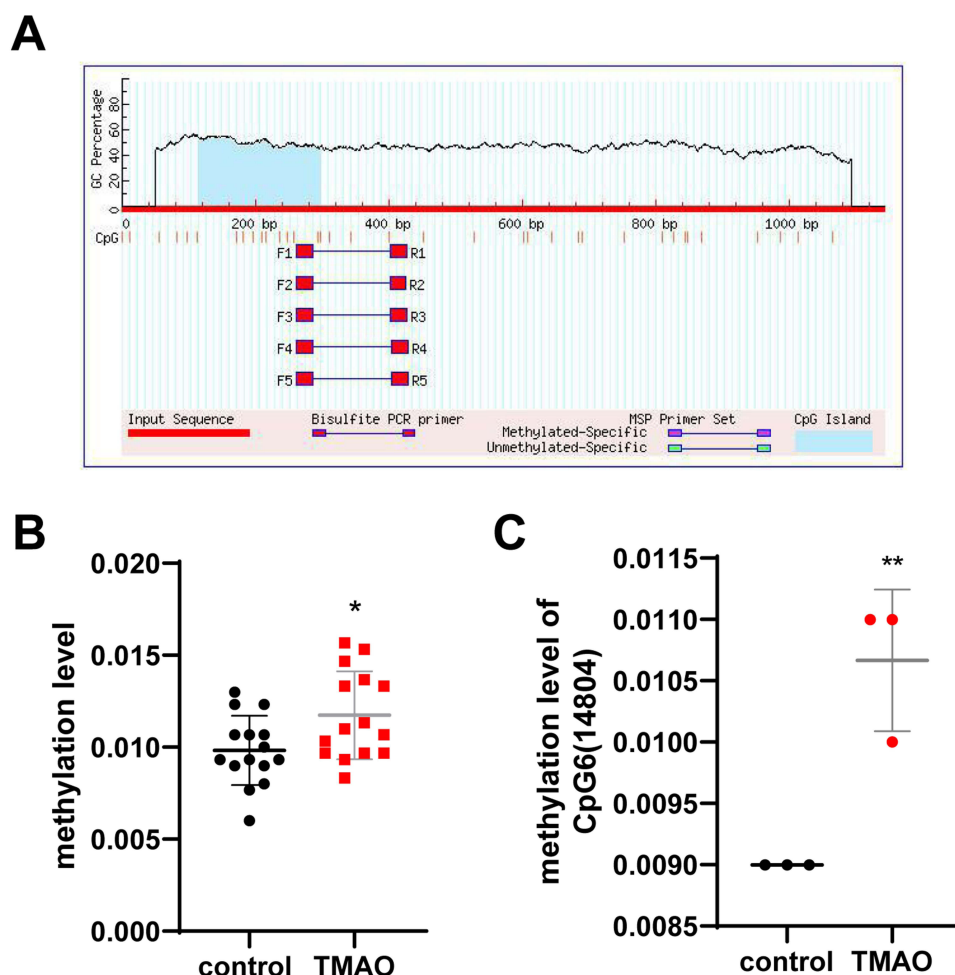


Figure 8 TMAO increases the methylation level of *CYTb* promoter: **(A)** The MethPrimer was used to analyze the CpG island. **(B)** Total average methylation level of 15 CpG gene. **(C)** The methylation level in the promoter region of CpG6 (14804) in the TMAO group was higher than that in the control group. * $P < 0.05$; ** $P < 0.01$ versus control group.

pyroptosis and MDF induced by TMAO were linked to the *CYTb* gene. *CYTb* overexpression inhibited TMAO-induced VECs pyroptosis, while inhibition of *CYTb* expression induced VECs pyroptosis, an effect that can be mitigated by targeting mitochondrial ROS with the inhibitor MitoTEMPO. Antioxidant MitoTEMPO can reduce the maturation of inflammatory cytokines, thus reducing TMAO-induced pyroptosis of endothelial cells.

DNA methylation modification is a form of epigenetic modification, which mainly occurs in CpG dinucleotides, and is usually related to gene suppression.⁶⁸ Recently, a CpG site in the mitochondrial gene *CYTb* has been identified,⁶⁹ and the expression level of *CYTb* is related to mtDNA methylation.⁷⁰ This is consistent with this research results, CpG islands were found in the promoter of the *CYTb* gene by bioinformatics analysis. In this study, mtDNA methylation was detected by TBS analysis, which found that the methylation level of *CYTb* promoter increased at the overall level and site 14804 after TMAO treatment, VECs pyroptosis induced by TMAO was related to hypermethylation of *CYTb*, indicating that there may be methylation regulation sites in the *CYTb* gene. However, mitochondrial genes are predominantly regulated by the D-loop region, and therefore, the methylation status of the D-loop should be assessed in future studies.

Demethylase TET2 can catalyze the oxidation of 5-mc in DNA into 5-hmC and inhibit the development of AS.^{34,42} The deficiency of TET2 leads to the increase of ROS production and disruption of mitochondrial dynamic balance.⁷¹ Moreover, the secretion of IL-1 β and the activity of NLRP3 inflammatory body are enhanced by TET2 inactivation.⁷² Our previous studies have shown that TET2 silencing can induce VECs pyroptosis by promoting the production of ROS

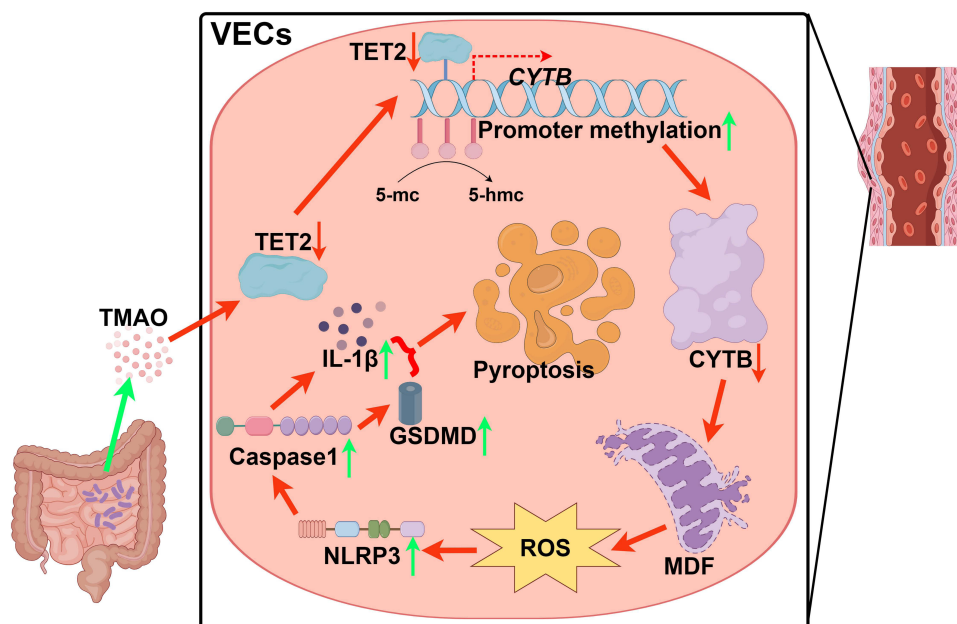


Figure 9 Mechanisms of TET2-CYTB-ROS pathway activated by TMAO induces vascular endothelial cells pyroptosis: TMAO produced by gut flora inhibits TET2 expression. The down-regulated TET2 promotes the methylation level of the *CYTB* gene promoter, which causes decreased *CYTB* transcription (indicated by red dashed lines). The decreased expression of *CYTB* resulted in MDF, ROS generation, activation of NLRP3 and Caspase-1, and upregulation of IL-1 β and GSDMD, eventually causing VECs pyroptosis.

in VECs.^{35,36} In this study, TMAO can down-regulate the expression of TET2, which suppresses the expression of *CYTB*. Interfering with TET2 can regulate the expression of *CYTB*. Therefore, this study showed that TET2 was involved in TMAO-induced VECs pyroptosis through regulation of *CYTB* methylation. However, TET2 enters mitochondrial and regulation of *CYTB* is not completely clear, and further experiments are needed.

Overall, the results of this study showed that TMAO induced MDF and increased ROS production primarily by inhibiting TET2 and *CYTB*, which subsequently leads to VECs pyroptosis. Therefore, TET2 may protect against AS induced by oxidative stress through the demethylation of *CYTB*. Targeting *CYTB* to regulate mtDNA methylation could represent a novel therapeutic strategy for the intervention of AS.

In this study, by a series of in vitro experiments, we proved that TMAO inhibited the expression of TET2 and *CYTB*, induced MDF, and promoted the production of ROS, which led to pyroptosis of VECs. This study found a new mechanism by which TMAO promoted AS. However, several limitations were not resolved. First, there is no direct evidence supporting the role of *CYTB* in VECs pyroptosis, and the specific molecular mechanisms regulating *CYTB* require further investigation. Additionally, mitochondrial *CYTB* expression was not assessed directly, as mitochondria were not extracted for analysis. Although TET2's impact on mitochondrial function has been suggested, the precise role and mechanism by which TET2 regulates *CYTB* demethylation should be further explored in vivo. Moreover, we did not perform methylation sequencing to confirm whether *CYTB* expression is regulated by TET2 at the methylation level, nor did we evaluate the effect of TET2 on the methylation of other mitochondrial factors. In the future, in vivo experiments are expected to provide more reliable evidence to support the TET2-CYTB-ROS pathway in VECs pyroptosis.

Conclusion

In this study, we found that TET2 and *CYTB* down-regulated by TMAO resulted in MDF, ROS generation, NLRP3 and Caspase-1 activation, and eventually led to VECs pyroptosis (Figure 9). In addition, after the down-regulation of TET2, the methylation of mtDNA was abnormal, and then the regulation of *CYTB* expression led to MDF. This study proved that *CYTB* is regulated by TET2 demethylation modification. Therefore, *CYTB* can inhibit TMAO induced VECs pyroptosis, which is expected to become a new target for the treatment of AS.

Data Sharing Statement

The data that supports the findings of this study are available in this article.

Ethics Approval

Ethical approval for our study was granted by Ethics Committee of Hunan Normal University (No. 2024601).

Acknowledgments

We thank all the people who offer help for this study. Co-Correspondence authors: Zuo Wang and Xiangyu Chen contributed equally to this paper. Co-first affiliations: Changsha Hospital for Maternal and Child Health Care, Hunan Normal University and Hengyang Medical School, University of South China contributed equally to this paper.

Author Contributions

All authors made a significant contribution to the work reported, whether that is in the conception, study design, execution, acquisition of data, analysis and interpretation, or in all these areas; took part in drafting, revising or critically reviewing the article; gave final approval of the version to be published; have agreed on the journal to which the article has been submitted; and agree to be accountable for all aspects of the work.

Funding

This study was supported by the Natural Science Foundation of China (81970389), the Natural Science Foundation of Hunan Province (2025JJ60670, 2024JJ9395, and 2025JJ70171) and the Natural Science Foundation of Changsha, China (kq2403186).

Disclosure

The authors report no conflicts of interest in this work.

References

- Libby P. The changing landscape of atherosclerosis. *Nature*. 2021;592(7855):524–533. doi:10.1038/s41586-021-03392-8
- Mathur P, Ostadal B, Romeo F, Mehta JL. Gender-Related Differences in Atherosclerosis. *Cardiovasc Drugs Ther*. 2015;29(4):319–327. doi:10.1007/s10557-015-6596-3
- WHO. Global Health Estimates 2021: deaths by Cause, Age, Sex, by Country and by Region, 2000–2021, Available from: <https://www.who.int/data/global-health-estimates>. Accessed Jun 26, 2025.
- Zhao D, Liu J, Wang M, Zhang X, Zhou M. Epidemiology of cardiovascular disease in China: current features and implications. *Nat Rev Cardiol*. 2019;16(4):203–212. doi:10.1038/s41569-018-0119-4
- Wang ZT, Wang Z, Hu YW. Possible roles of platelet-derived microparticles in atherosclerosis. *Atherosclerosis*. 2016;248:10–16. doi:10.1016/j.atherosclerosis.2016.03.004
- Liu X, Luo P, Zhang W, Zhang S, Yang S, Hong F. Roles of pyroptosis in atherosclerosis pathogenesis. *Biomed Pharmacother*. 2023;166:115369. doi:10.1016/j.biopha.2023.115369
- Man SM, Karki R, Kanneganti TD. Molecular mechanisms and functions of pyroptosis, inflammatory caspases and inflammasomes in infectious diseases. *Immunol Rev*. 2017;277(1):61–75. doi:10.1111/imr.12534
- Tang R, Xu J, Zhang B, et al. Ferroptosis, necroptosis, and pyroptosis in anticancer immunity. *J Hematol Oncol*. 2020;13(1):110. doi:10.1186/s13045-020-00946-7
- Wang Q, Wu J, Zeng Y, et al. Pyroptosis: a pro-inflammatory type of cell death in cardiovascular disease. *Clin Chim Acta*. 2020;510:62–72. doi:10.1016/j.cca.2020.06.044
- Miao R, Jiang C, Chang WY, et al. Gasdermin D permeabilization of mitochondrial inner and outer membranes accelerates and enhances pyroptosis. *Immunity*. 2023;56(11):2523–2541.e2528. doi:10.1016/j.immuni.2023.10.004
- Robinson N, Ganesan R, Hegedüs C, Kovács K, Kufer TA, Virág L. Programmed necrotic cell death of macrophages: focus on pyroptosis, necroptosis, and parthanatos. *Redox Biol*. 2019;26:101239. doi:10.1016/j.redox.2019.101239
- Zhang J, Dai Y, Yang Y, Xu J. Calcitriol Alleviates Hyperosmotic Stress-Induced Corneal Epithelial Cell Damage via Inhibiting the NLRP3-ASC-Caspase-1-GSDMD Pyroptosis Pathway in Dry Eye Disease. *J Inflamm Res*. 2021;14:2955–2962. doi:10.2147/jir.S310116
- Schwartz EA, Reaven PD. Lipolysis of triglyceride-rich lipoproteins, vascular inflammation, and atherosclerosis. *Biochim Biophys Acta*. 2012;1821(5):858–866. doi:10.1016/j.bbalip.2011.09.021
- Vallance HD, Koochin A, Branov J, et al. Marked elevation in plasma trimethylamine-N-oxide (TMAO) in patients with mitochondrial disorders treated with oral l-carnitine. *Mol Genet Metab Rep*. 2018;15:130–133. doi:10.1016/j.ymgmr.2018.04.005
- Wang Z, Klipfell E, Bennett BJ, et al. Gut flora metabolism of phosphatidylcholine promotes cardiovascular disease. *Nature*. 2011;472(7341):57–63. doi:10.1038/nature09922

16. Li J, Lü H, Chen S, Xiang H, Zhao S, Zhao S. Trimethylamine oxide induces pyroptosis of vascular endothelial cells through ALDH2/ROS/NLRP3/GSDMD pathway. *Zhong Nan Da Xue Xue Bao Yi Xue Ban*. 2022;47(9):1171–1181. doi:10.11817/j.issn.1672-7347.2022.220086
17. Wu P, Chen J, Chen J, et al. Trimethylamine N-oxide promotes apoE(-/-) mice atherosclerosis by inducing vascular endothelial cell pyroptosis via the SDHB/ROS pathway. *J Cell Physiol*. 2020;235(10):6582–6591. doi:10.1002/jcp.29518
18. Chen J, Zhang J, Wu J, et al. Low shear stress induced vascular endothelial cell pyroptosis by TET2/SDHB/ROS pathway. *Free Radic Biol Med*. 2021;162:582–591. doi:10.1016/j.freeradbiomed.2020.11.017
19. Ji F, Zhao C, Wang B, Tang Y, Miao Z, Wang Y. The role of 5-hydroxymethylcytosine in mitochondria after ischemic stroke. *J Neurosci Res*. 2018;96(10):1717–1726. doi:10.1002/jnr.24274
20. Jiang X, Ma C, Gao Y, et al. Tongxinluo attenuates atherosclerosis by inhibiting ROS/NLRP3/caspase-1-mediated endothelial cell pyroptosis. *J Ethnopharmacol*. 2023;304:116011. doi:10.1016/j.jep.2022.116011
21. Qiu Z, He Y, Ming H, Lei S, Leng Y, Xia ZY. Lipopolysaccharide (LPS) Aggravates High Glucose- and Hypoxia/Reoxygenation-Induced Injury through Activating ROS-Dependent NLRP3 Inflammasome-Mediated Pyroptosis in H9C2 Cardiomyocytes. *J Diabetes Res*. 2019;2019:8151836. doi:10.1155/2019/8151836
22. Hagen CM, Aidt FH, Havndrup O, et al. MT-CYB mutations in hypertrophic cardiomyopathy. *Mol Genet Genomic Med*. 2013;1(1):54–65. doi:10.1002/mgg3.5
23. Kirchhoff H, Li M, Puthiyaveetil S. Sublocalization of Cytochrome b(6)f Complexes in Photosynthetic Membranes. *Trends Plant Sci*. 2017;22(7):574–582. doi:10.1016/j.tplants.2017.04.004
24. Mohammad G, Kumar J, Kowluru RA. Mitochondrial Genome-Encoded Long Noncoding RNA Cytochrome B and Mitochondrial Dysfunction in Diabetic Retinopathy. *Antioxid Redox Signal*. 2023;39(13–15):817–828. doi:10.1089/ars.2023.0303
25. Tucker EJ, Wanschers BF, Szklarczyk R, et al. Mutations in the UQCRC1-interacting protein, UQCRC2, cause human complex III deficiency associated with perturbed cytochrome b protein expression. *PLoS Genet*. 2013;9(12):e1004034. doi:10.1371/journal.pgen.1004034
26. Valnot I, Kassiss J, Chretien D, et al. A mitochondrial cytochrome b mutation but no mutations of nuclearly encoded subunits in ubiquinol cytochrome c reductase (complex III) deficiency. *Hum Genet*. 1999;104(6):460–466. doi:10.1007/s004390050988
27. Cordero MD, Alcocer-Gómez E, Marín-Aguilar F, et al. Mutation in cytochrome b gene of mitochondrial DNA in a family with fibromyalgia is associated with NLRP3-inflammasome activation. *J Med Genet*. 2016;53(2):113–122. doi:10.1136/jmedgenet-2015-103392
28. Dasgupta S, Hoque MO, Upadhyay S, Sidransky D. Forced cytochrome B gene mutation expression induces mitochondrial proliferation and prevents apoptosis in human uroepithelial SV-HUC-1 cells. *Int J Cancer*. 2009;125(12):2829–2835. doi:10.1002/ijc.24701
29. Osmenda G, Matusik PT, Sliwa T, et al. Nicotinamide adenine dinucleotide phosphate (NADPH) oxidase p22phox subunit polymorphisms, systemic oxidative stress, endothelial dysfunction, and atherosclerosis in type 2 diabetes mellitus. *Pol Arch Intern Med*. 2021;131(5):447–454. doi:10.20452/pamw.15937
30. Pal A, Pal A, Banerjee S, Batabyal S, Chatterjee PN. Mutation in Cytochrome B gene causes debility and adverse effects on health of sheep. *Mitochondrion*. 2019;46:393–404. doi:10.1016/j.mito.2018.10.003
31. Śmiech A, Ślaska B, Bownik A, Grzybowska-Szatowska L, Dudka J, Łopuszyński W. Heteroplasmic Mutations and Polymorphisms in the Cyb Gene of Mitochondrial DNA in Canine Mast Cell Tumours. *Vivo*. 2019;33(1):57–63. doi:10.21873/invivo.11439
32. Sobenin IA, Zhelankin AV, Khasanova ZB, et al. Heteroplasmic Variants of Mitochondrial DNA in Atherosclerotic Lesions of Human Aortic Intima. *Biomolecules*. 2019;9(9):455. doi:10.3390/biom9090455
33. Xu Z, Mo Y, Li X, et al. The Novel LncRNA AK035396 Drives Cardiomyocyte Apoptosis Through Mterf1 in Myocardial Ischemia/Reperfusion Injury. *Front Cell Dev Biol*. 2021;9:773381. doi:10.3389/fcell.2021.773381
34. Ko M, Huang Y, Jankowska AM, et al. Impaired hydroxylation of 5-methylcytosine in myeloid cancers with mutant TET2. *Nature*. 2010;468(7325):839–843. doi:10.1038/nature09586
35. Chen JJ, Tao J, Zhang XL, et al. Inhibition of the ox-LDL-Induced Pyroptosis by FGF21 of Human Umbilical Vein Endothelial Cells Through the TET2-UQCRC1-ROS Pathway. *DNA Cell Biol*. 2020;39(4):661–670. doi:10.1089/dna.2019.5151
36. ZhaoLin Z, Jiaojiao C, Peng W, et al. OxLDL induces vascular endothelial cell pyroptosis through miR-125a-5p/TET2 pathway. *J Cell Physiol*. 2019;234(5):7475–7491. doi:10.1002/jcp.27509
37. Singh GB, Zhang Y, Boini KM, Koka S. High Mobility Group Box 1 Mediates TMAO-Induced Endothelial Dysfunction. *Int J Mol Sci*. 2019;20(14):3570. doi:10.3390/ijms20143570
38. Chen Y, Yuan C, Qin W, Yu B, Wei D, Wu P. TMAO promotes vascular endothelial cell pyroptosis via the LPEAT-mitophagy pathway. *Biochem Biophys Res Commun*. 2024;703:149667. doi:10.1016/j.bbrc.2024.149667
39. Miao EA, Rajan JV, Aderem A. Caspase-1-induced pyroptotic cell death. *Immunol Rev*. 2011;243(1):206–214. doi:10.1111/j.1600-065X.2011.01044.x
40. Zhou R, Yazdi AS, Menu P, Tschopp J. A role for mitochondria in NLRP3 inflammasome activation. *Nature*. 2011;469(7329):221–225. doi:10.1038/nature09663
41. Grzybowska-Szatowska L, Ślaska B. Mitochondrial DNA and carcinogenesis (review). *Mol Med Rep*. 2012;6(5):923–930. doi:10.3892/mmr.2012.1027
42. Jiang D, Sun M, You L, et al. DNA methylation and hydroxymethylation are associated with the degree of coronary atherosclerosis in elderly patients with coronary heart disease. *Life Sci*. 2019;224:241–248. doi:10.1016/j.lfs.2019.03.021
43. Joshi SR, Kitagawa A, Jacob C, et al. Hypoxic activation of glucose-6-phosphate dehydrogenase controls the expression of genes involved in the pathogenesis of pulmonary hypertension through the regulation of DNA methylation. *Am J Physiol Lung Cell Mol Physiol*. 2020;318(4):L773–L786. doi:10.1152/ajplung.00001.2020
44. Liu R, Chen L, Wang Z, et al. Downregulation of the DNA 5-hydroxymethylcytosine is involved in mitochondrial dysfunction and neuronal impairment in high fat diet-induced diabetic mice. *Free Radic Biol Med*. 2020;148:42–51. doi:10.1016/j.freeradbiomed.2019.12.042
45. Welsh P, Grassia G, Botha S, Sattar N, Maffia P. Targeting inflammation to reduce cardiovascular disease risk: a realistic clinical prospect? *Br J Pharmacol*. 2017;174(22):3898–3913. doi:10.1111/bph.13818
46. Liu Z, Wang C, Lin C. Pyroptosis as a double-edged sword: the pathogenic and therapeutic roles in inflammatory diseases and cancers. *Life Sci*. 2023;318:121498. doi:10.1016/j.lfs.2023.121498
47. Ji N, Qi Z, Wang Y, et al. Pyroptosis: a New Regulating Mechanism in Cardiovascular Disease. *J Inflamm Res*. 2021;14:2647–2666. doi:10.2147/jir.S308177

48. Shanmugham M, Devasia AG, Chin YL, et al. Time-dependent specific molecular signatures of inflammation and remodelling are associated with trimethylamine-N-oxide (TMAO)-induced endothelial cell dysfunction. *Sci Rep*. 2023;13(1):20303. doi:10.1038/s41598-023-46820-7
49. Vourakis M, Mayer G, Rousseau G. The Role of Gut Microbiota on Cholesterol Metabolism in Atherosclerosis. *Int J Mol Sci*. 2021;22(15):8074. doi:10.3390/ijms22158074
50. Jonsson AL, Bäckhed F. Role of gut microbiota in atherosclerosis. *Nat Rev Cardiol*. 2017;14(2):79–87. doi:10.1038/nrcardio.2016.183
51. Wang B, Qiu J, Lian J, Yang X, Zhou J. Gut Metabolite Trimethylamine-N-Oxide in Atherosclerosis: from Mechanism to Therapy. *Front Cardiovasc Med*. 2021;8:723886. doi:10.3389/fcvm.2021.723886
52. Lopez-Pastrana J, Ferrer LM, Li YF, et al. Inhibition of Caspase-1 Activation in Endothelial Cells Improves Angiogenesis: a NOVEL THERAPEUTIC POTENTIAL FOR ISCHEMIA. *J Biol Chem*. 2015;290(28):17485–17494. doi:10.1074/jbc.M115.641191
53. Wu X, Zhang H, Qi W, et al. Nicotine promotes atherosclerosis via ROS-NLRP3-mediated endothelial cell pyroptosis. *Cell Death Dis*. 2018;9(2):171. doi:10.1038/s41419-017-0257-3
54. Wang X, Bian Y, Zhang R, et al. Melatonin alleviates cigarette smoke-induced endothelial cell pyroptosis through inhibiting ROS/NLRP3 axis. *Biochem Biophys Res Commun*. 2019;519(2):402–408. doi:10.1016/j.bbrc.2019.09.005
55. Hu Z, Yang L, Zhang M, et al. A novel protein CYTB-187AA encoded by the mitochondrial gene CYTB modulates mammalian early development. *Cell Metab*. 2024;36(7):1586–1597.e1587. doi:10.1016/j.cmet.2024.04.012
56. Xia D, Yu CA, Kim H, et al. Crystal structure of the cytochrome bc1 complex from bovine heart mitochondria. *Science*. 1997;277(5322):60–66. doi:10.1126/science.277.5322.60
57. Song Z, Laleve A, Vallières C, McGeehan JE, Lloyd RE, Meunier B. Human Mitochondrial Cytochrome b Variants Studied in Yeast: not All Are Silent Polymorphisms. *Hum Mutat*. 2016;37(9):933–941. doi:10.1002/humu.23024
58. Chiu JE, Renard I, George S, et al. Cytochrome b Drug Resistance Mutation Decreases Babesia Fitness in the Tick Stages But Not the Mammalian Erythrocytic Cycle. *J Infect Dis*. 2022;225(1):135–145. doi:10.1093/infdis/jiab321
59. De Coo IF, Renier WO, Ruitenbeek W, et al. A 4-base pair deletion in the mitochondrial cytochrome b gene associated with parkinsonism/MELAS overlap syndrome. *Ann Neurol*. 1999;45(1):130–133. doi:10.1002/1531-8249(199901)45:1<130::aid-art21>3.3.co;2-q
60. Keightley JA, Anitori R, Burton MD, Quan F, Buist NR, Kennaway NG. Mitochondrial encephalomyopathy and complex III deficiency associated with a stop-codon mutation in the cytochrome b gene. *Am J Hum Genet*. 2000;67(6):1400–1410. doi:10.1086/316900
61. Mancuso M. Complex neurological and multisystem presentations in mitochondrial disease. *Handb Clin Neurol*. 2023;194:117–124. doi:10.1016/b978-0-12-821751-1.00003-8
62. Nikitin AG, Lavrikova EY, Chistiakov DA. The heteroplasmic 15059G>A mutation in the mitochondrial cytochrome b gene and essential hypertension in type 2 diabetes. *Diabetes Metab Syndr*. 2012;6(3):150–156. doi:10.1016/j.dsx.2012.09.005
63. Schuelke M, Krude H, Finckh B, et al. Septo-optic dysplasia associated with a new mitochondrial cytochrome b mutation. *Ann Neurol*. 2002;51(3):388–392. doi:10.1002/ana.10151
64. Sobenin IA, Chistiakov DA, Sazonova MA, et al. Association of the level of heteroplasmy of the 15059G>A mutation in the MT-CYB mitochondrial gene with essential hypertension. *World J Cardiol*. 2013;5(5):132–140. doi:10.4330/wjc.v5.i5.132
65. Zarrouk Mahjoub S, Mehri S, Ourda F, Finsterer J, Ben Arab S. Novel m.15434C>A (p.230L>I) Mitochondrial Cytb Gene Missense Mutation Associated with Dilated Cardiomyopathy. *ISRN Cardiol*. 2012;2012:251723. doi:10.5402/2012/251723
66. Hahn A, Zuryin S. Mitochondrial Genome (mtDNA) Mutations that Generate Reactive Oxygen Species. *Antioxidants (Basel)*. 2019;8(9). doi:10.3390/antiox8090392
67. Sobenin IA, Sazonova MA, Postnov AY, Bobryshev YV, Orekhov AN. Mitochondrial mutations are associated with atherosclerotic lesions in the human aorta. *Clin Dev Immunol*. 2012;2012:832464. doi:10.1155/2012/832464
68. Peng J, Tang ZH, Ren Z, et al. TET2 Protects against oxLDL-Induced HUVEC Dysfunction by Upregulating the CSE/H(2)S System. *Front Pharmacol*. 2017;8:486. doi:10.3389/fphar.2017.00486
69. Kowal K, Tkaczyk A, Ząbek T, Pierzchała M, Ślaska B. Comparative Analysis of CpG Sites and Islands Distributed in Mitochondrial DNA of Model Organisms. *Animals*. 2020;10(4). doi:10.3390/ani10040665
70. Liu B, Du Q, Chen L, et al. CpG methylation patterns of human mitochondrial DNA. *Sci Rep*. 2016;6(1):23421. doi:10.1038/srep23421
71. Herzig S, Shaw RJ. AMPK: guardian of metabolism and mitochondrial homeostasis. *Nat Rev Mol Cell Biol*. 2018;19(2):121–135. doi:10.1038/nrm.2017.95
72. Fuster JJ, MacLauchlan S, Zuriaga MA, et al. Clonal hematopoiesis associated with TET2 deficiency accelerates atherosclerosis development in mice. *Science*. 2017;355(6327):842–847. doi:10.1126/science.aag1381